Multilayer LTCC Bandpass Filter Design With Enhanced Stopband Characteristics

Wing-Yan Leung, Kwok-Keung M. Cheng, *Member, IEEE*, and Ke-Li Wu, *Senior Member, IEEE*

***Abstract*—Lumped-element bandpass filter structures with enhanced stopband rejection targeted for low temperature co-fired ceramic (LTCC) implementation are proposed. Design equation formulations that take into account the effect of the transmission zeros are presented. For demonstration, RF filters operating at 2.4 GHz are fabricated and characterized. Both simulation and measurement results are shown for comparison.**

***Index Terms*—Filters, lumped-element, multilayer.**

I. Introduction

MICROWAVE filters are an essential component in modern wireless communication systems. In transceiver designs, RF bandpass filters are sometimes required for the separation of the uplink and downlink transmission paths. Narrow-band filters are also used for the rejection of the image channel, as well as any strong interfering signals in nearby frequency band. Such devices may be realized by using SAW technology in mobile communications. Recently, the use of low temperature co-fired ceramic (LTCC) technology [1] in RF circuit design has become more popular due to its high performance, high integration density, and high reliability. LTCC is a multilayer ceramic technology, which provides an ability to embed passive components in layers while the active elements are mounted on the surface layer. This paper describes the design and construction of RF bandpass filters suitable for integration in a LTCC miniaturized transceiver module.

II. Filter Design

The design of RF filters is quite a challenging task. The stopband characteristics of the filters are a prime factor in determining the isolation between the transmitting and receiving paths in duplexer designs [2]. It is well known that the stopband rejection may be enhanced, either by increasing the number of resonators [3], or by adding transmission zeros [4]. Fig. 1 shows the lumped-element circuit topologies that can be used to realize a second-order bandpass filter with two transmission zeros located at arbitrary frequencies. Basically, there are three possible types of filter characteristics depending on the frequency range of the transmission zeros in relation to the passband. For example, the configurations shown in Fig. 1(a) and (b) can be used to realize ISM-band filters (2.45 GHz) with a much higher attenuation level in the lower stopband for the rejection of the image channel, as well as any strong interfering signals that may appear in the PCS and GSM bands.

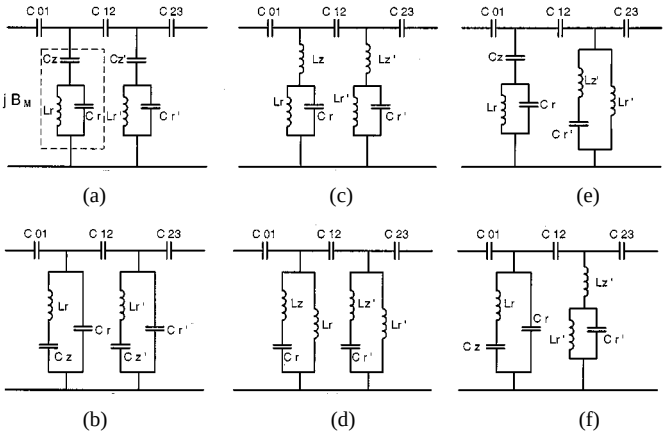

Fig. 1. Bandpass filters with transmission zeros located at pre-selected frequency values. (a)–(b) Both zeros are located at the lower stopband; (c)–(d) both zeros are located at the upper stopband; (e)–(f) zeros are located at both the lower and upper stopbands.

Design equations for calculating the element values of the proposed filter structures can be derived by using the standard filter synthesis procedures [3] in conjunction with the following conditions:

$$B_M(\omega=\omega_z)=\infty \tag{1a}$$

$$B_M(\omega=\omega_0)=B_S(\omega=\omega_0) \tag{1b}$$

$$\left.\frac{dB_M(\omega)}{d\omega}\right|_{\omega=\omega_0}=\left.\frac{dB_S(\omega)}{d\omega}\right|_{\omega=\omega_0} \tag{1c}$$

where ω_0 and ω_z are the passband center frequency and the transmission zero frequency, respectively; B_M and B_S are the admittances of the resonators associated with the proposed and standard filter configurations, respectively. For the particular circuits shown in Fig. 1(e), the component values are simply given by

$$C_{12}=\frac{C_S}{\sqrt{2}}\cdot\frac{BW}{\omega_o} \tag{2a}$$

$$C_{01}=C_{23}=\frac{1}{\omega_o Z_o}\sqrt{\frac{\omega_o C_{12} Z_o}{1-\omega_o C_{12} Z_o}} \tag{2b}$$

$$L_r=\frac{1}{C_{eff}}\cdot\frac{\omega_{z1}^2-\omega_p^2}{\omega_p^4}\cdot\frac{\omega_o^2-\omega_p^2}{\omega_o^2-\omega_{z1}^2} \tag{2c}$$

$$C_r=\frac{1}{\omega_p^2 L_r} \tag{2d}$$

Manuscript received October 31, 2001; revised April 22, 2002. The review of this letter was arranged by Associate Editor Rüdiger Vahldieck.

The authors are with the Department of Electronic Engineering, Chinese University of Hong Kong, Shatin, Hong Kong.

Publisher Item Identifier 10.1109/LMWC.2002.801130.

$$C_z = \frac{1}{L_r}\left(\frac{1}{\omega_{z1}^2} - \frac{1}{\omega_p^2}\right) \tag{2e}$$

$$L_r' = \left[\frac{1}{L_z'\left(\frac{\omega_{z2}}{\omega_o}\right)^2 - 1} - \omega_o^2 C_{eff}\right]^{-1} \tag{2f}$$

$$C_r' = \frac{1}{\omega_{z2}^2 L_z'} \tag{2h}$$

$$L_z' = \frac{\omega_{z2}^2}{C_S(\omega_o^2 - \omega_{z2}^2)^2} \tag{2i}$$

where

$$\omega_p = \frac{(1-k)\omega_o^4 + (k-3)\omega_o^2\omega_{z1}^2}{(k-1)\omega_{z1}^2 - (k+1)\omega_o^2}$$

$$k = \frac{-2C_S}{C_{eff}}$$

$$C_{eff} = C_{01} + C_{12} - \omega_o C_{01} C_{12} Z_o.$$

BW is the 3 dB bandwidth; C_S is the shunt capacitors of the resonators associated with the standard filter design; ω_{z1} and ω_{z2} are, respectively, the frequency values of the transmission zeroes located at the lower and upper stopbands.

III. LTCC Filter Implementation

For illustration, 2.4 GHz RF filters based on the circuit configurations shown in Fig. 1(a) and (e) are designed and realized using LTCC technology. First of all, the lumped-element values are evaluated by the derived equations and verified by using a circuit simulator. After that, individual components are replaced by the corresponding layout based on the design rules and data provided by the LTCC foundry. The capacitors used are all parallel-plate type and the dimensions are obtained by using the Moment Method. Inductors are either strip- or spiral-shaped, depending on the amount of inductance required. Dimensions of these inductors are determined by the formula described in [5], [6].

Due to the close proximity between components within the LTCC structure, the mutual coupling associated with the physical layout may corrupt the filter performance. As a result, the electrical characteristics of the complete layout including the parasitic effect of via conductors are examined by using a full-wave electromagnetic simulation package. Further modifications are made in two steps. Manual tuning is first applied to obtain a filter with some reasonable performance, either by changing the positions and dimensions of individual components or by placing the components in different layers. Then, the layout was fine-tuned by using the optimization function provided by the software package. Insertion loss within the passband and the amount of attenuation in the stopband are used as the targets, whereas the dimensions of the components are selected as the optimizing parameters. Fig. 2 shows the physical view of the final layout design.

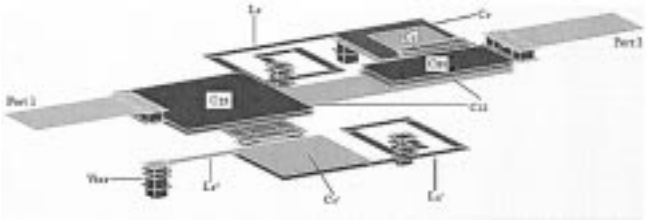

Fig. 2. Layout of the LTCC filter in 3-D view.

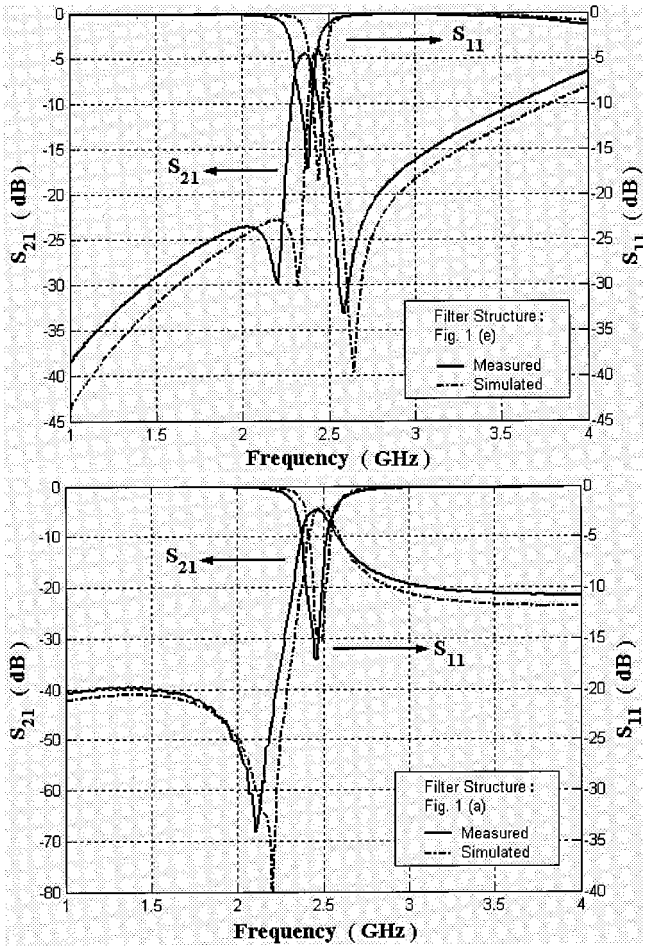

Fig. 3. Simulated and measured frequency responses of the LTCC filter.

IV. Measurements and Discussions

All the components of the filter were embedded in an LTCC substrate (DuPont 951 tape) with a relative dielectric constant and loss tangent of 7.8 and 0.001, respectively. All the embedded conductors are silver while the surface layer conductors are silver/palladium alloy. The prototype was fabricated by the National Semiconductor Corporation and has a dimension of roughly 215 mils by 100 mils. Measurements were carried out using a HP8510C Network Analyzer and a Summit 9000 Probe Station. To ensure high measurement accuracy, a two-tier calibration procedure is adopted here.

For illustration, both the measured transmission and input reflection responses of the constructed filters are plotted in Fig. 3. According to the measurement results, the prototype filter circuit upper diagram exhibits a center frequency of 2.37 GHz, an

insertion loss of about 4.2 dB, and a 3 dB bandwidth of approximately 110 MHz. The diagram clearly indicates that the amount of attenuation close to the passband is greatly enhanced by the introduction of the transmission zeros. Good agreement between the predicted and measured results is observed. The small discrepancies between the two sets of data are mainly due to the finite thickness of the embedded conductors that has not been included in the electromagnetic simulation.

ACKNOWLEDGMENT

The authors would like to thank National Semiconductor Corporation for the technical support and LTCC Prototyping.

REFERENCES

[1] C. Q. Scrantom and J. C. Lawson, "LTCC technology: Where we are and where we're going—II," in *IEEE Int. Microwave Symp. Dig.*, 1998, pp. 193–200.

[2] J. W. Sheen, "LTCC-MLC duplexer for DCS-1800," *IEEE Trans. Microwave Theory Tech.*, vol. 47, pp. 1883–1890, Sept. 1999.

[3] G. L. Matthaei, L. Young, and E. M. T. Jones, *Microwave Filter, Impedance-Matching Networks, and Coupling Structures*. New York: McGraw-Hill, 1964, ch. 8.

[4] J. S. Lim and D. C. Park, "A modified Chebyshev bandpass filter with attenuation poles in the stopband," *IEEE Trans. Microwave Theory Tech.*, vol. 45, pp. 898–904, June 1997.

[5] C. Hoer and C. Love, "Exact inductance equations for rectangular conductors with applications to more complicated geometries," *J. Res. Nat. Bur. Stand. C, Eng. Instrum.*, vol. 69, no. 2, pp. 127–137, Apr.–June 1965.

[6] B. C. Wadell, *Transmission Line Design Handbook*. Boston, MA: Artech House, 1991, pp. 399–402.